







Article

Auxin-Amido Synthetase Gene *ThGH3.1* Regulates Auxin Levels to Suppress Root Development in Transgenic *Arabidopsis* and *Tetrastigma hemsleyanum* Hairy Roots

Xiaoping Huang^{1,*}, Hao Yu¹, Jie Jiang¹, Ruyi Zheng¹, Fangzhen Li², Zhiming Yu¹, Zhanghui Zeng¹, Zhehao Chen¹, Tao Chen¹, Lilin Wang¹ and Taihe Xiang¹

¹ College of Life and Environmental Sciences, Hangzhou Normal University, Hangzhou 311121, China; 2023111010051@stu.hznu.edu.cn (H.Y.); 2022111010001@stu.hznu.edu.cn (J.J.); 2023210304063@stu.hznu.edu.cn (R.Z.); yuzhiming@hznu.edu.cn (Z.Y.); zhzheng@hznu.edu.cn (Z.Z.); zhchen@hznu.edu.cn (Z.C.); chentao@hznu.edu.cn (T.C.); llwang@hznu.edu.cn (L.W.); xthcn@hznu.edu.cn (T.X.)

² Institute of Resources and Environment, Shaoxing Academy of Agricultural Sciences, Shaoxing 312003, China; lifzhen@163.com

* Correspondence: xphuang@hznu.edu.cn

Abstract

Tetrastigma hemsleyanum Diels et Gilg (*T. hemsleyanum*) is a prized Chinese medicinal plant renowned for its medicinal and economic importance. In our previous study, a key auxin-related gene *ThGH3.1* (encoding amide synthetase) was identified by quantitative transcriptome sequencing. To explore *ThGH3.1* function in root development, we generated *ThGH3.1*-overexpressing and RNA interference (RNAi) transgenic hairy root lines via *Agrobacterium rhizogenes* (*A. rhizogenes*)-mediated genetic transformation. The results showed that overexpression of *ThGH3.1* significantly inhibited the total length and the lateral root number of hairy roots, accompanied by significantly increased levels of methyl indole-3-acetate (MeIAA) and indole-3-acetyl-aspartate (IAA-Asp). In contrast, *ThGH3.1* knockdown displayed an opposite trend. To further confirm the function of *ThGH3.1*, the overexpression vector was heterologously transformed into wild-type *Arabidopsis*. After single-copy and homozygous line screening, three overexpressing lines (named G19, G29, and G32) were obtained. The primary root length of transgenic *Arabidopsis* was significantly shortened, with a significant increase in indole-3-acetonitrile (IAN) levels. Further pot experiments revealed that transgenic *Arabidopsis* grew more slowly, had significantly smaller leaf areas, and lower plant height. The indole-3-acetic acid (IAA) treatment suggested that *ThGH3.1* responded to IAA. Collectively, these findings highlight the crucial roles of *ThGH3.1* in regulating root development, which will deepen our understanding of the molecular mechanisms underlying root development in *T. hemsleyanum*.

Keywords: hairy roots; heterologous transformation; phytohormone levels; RNA interference; *Tetrastigma hemsleyanum*



Academic Editor: Alessandra Carrubba

Received: 2 November 2025

Revised: 8 December 2025

Accepted: 12 December 2025

Published: 14 December 2025

Citation: Huang, X.; Yu, H.; Jiang, J.; Zheng, R.; Li, F.; Yu, Z.; Zeng, Z.; Chen, Z.; Chen, T.; Wang, L.; et al.

Auxin-Amido Synthetase Gene *ThGH3.1* Regulates Auxin Levels to Suppress Root Development in Transgenic *Arabidopsis* and *Tetrastigma hemsleyanum* Hairy Roots.

Horticulturae 2025, 11, 1512.

<https://doi.org/10.3390/horticulturae11121512>

horticulturae11121512

Copyright: © 2025 by the authors.

Licensee MDPI, Basel, Switzerland.

This article is an open access article distributed under the terms and conditions of the Creative Commons Attribution (CC BY) license

(<https://creativecommons.org/licenses/by/4.0/>).

1. Introduction

Tetrastigma hemsleyanum Diels et Gilg (*T. hemsleyanum*) belongs to the genus *Tetrastigma* in the *Vitaceae* family and is mainly distributed in the regions south of the Yangtze River in China. The entire plant is medicinal, with the root tubers boasting the highest medicinal value. It has been reported to possess properties of clearing heat, detoxifying, reducing

inflammation, and alleviating pain, as well as anti-tumor effects, thus being praised as the “plant antibiotic” [1]. In recent years, with the rising market demand for *T. hemsleyanum*, the overexploitation of its wild resources has become increasingly severe. Furthermore, the root tubers of *T. hemsleyanum* develop slowly under natural conditions. Therefore, it is of great significance to decipher the molecular mechanism regulating its root development.

Undoubtedly, considerable research has also been conducted on *T. hemsleyanum*. For example, the evolutionary relationships of *T. hemsleyanum* from different geographical regions have been analyzed via transcriptome sequencing [2]. Effective internal reference genes were screened to analyze gene expression in *T. hemsleyanum* [3]. The anthocyanin biosynthesis pathway in *T. hemsleyanum* has been elucidated by integrating transcriptome and metabolome profiling [4]. In previous work from our laboratory, the effect of the rhizosphere soil microbial community on flavonoid content in *T. hemsleyanum* was analyzed [5]. The endophytic fungus TH26 can promote plant growth, up-regulate the expression of the *Th-exp* gene, and increase flavonoid content in *T. hemsleyanum* [6]. However, research on the development of root tubers in *T. hemsleyanum* remains limited.

It is well-known that plant root and stem tubers exhibit diverse morphologies, and their formation all initiate from underground precursor organs [7]. For example, studies have shown that buds on the underground stem tubers of *Solanum tuberosum* elongate into stolons. Once the plant accumulates a certain amount of organic matter, the stolons stop their longitudinal growth, and their tips begin to swell, eventually forming tubers [8]. The root tubers of *Ipomoea batatas* develop from adventitious roots growing from stem nodes, which undergo hardening and swelling [9]. Certainly, the formation of plant root and stem tubers is a complex biological process. It is regulated by both external environments and endogenous signals and involves interactions across multiple levels including hormone signaling [10,11]. For instance, overexpression of the auxin biosynthesis gene *YUCCA* inhibits tuber formation [12]. Overexpression of *IbSRD1* leads to the early enlargement of root tubers, and it is speculated that this gene regulates the initial growth of root tubers in an auxin-dependent manner [13,14]. Particularly, a number of auxin-related genes encoding amide synthetase have been implicated in regulating root development [15].

The *GH3* (*Gretchen Hagen 3*) gene encodes an amide synthetase, a key enzyme in auxin metabolism. Several studies have reported the spatiotemporal specificity of *GH3* gene expression across different species. For example, the *MdGH3-4* gene is specifically up-regulated in apple roots [16]. The *BoGH3.13-1* gene is specifically expressed in the flower buds of cabbage plants [17]. In sugarcane, the *ScGH3-1* gene exhibits the lowest expression levels in roots and epidermis, and the highest in stems [18]. Additionally, numerous studies have documented the roles of *GH3* genes in plant root development, including in *Arabidopsis* [19–23]. For instance, the primary root length of *Arabidopsis AtGH3.9-RNAi* lines significantly increases compared with that of the wild type [24]. Overexpression of the *OsGH3* gene leads to reduced numbers of lateral roots and adventitious roots, with primary root growth also inhibited [25–28]. The tomato *SIGH3.15* gene negatively regulates the number of primary and lateral roots by modulating auxin homeostasis [29]. Overexpression of the *MsGH3.5* gene inhibits the development of buds and roots, ultimately resulting in dwarfism and fewer adventitious roots [30]. Overexpression of the tea plant *CsGH3.4* gene significantly reduces the number of adventitious roots in transgenic *Arabidopsis* [31]. However, no studies on the function of *ThGH3.1* genes in *T. hemsleyanum* have been reported so far.

In our previous study, digital transcriptome sequencing was performed on three different root forms of *T. hemsleyanum*, and we identified a key auxin-related gene *ThGH3.1* encoding amide synthetase [32]. To explore *ThGH3.1* function in root development, transgenic lines were generated using an *Agrobacterium rhizogenes* (*A. rhizogenes*)-mediated

genetic transformation and heterologous transformation system. Finally, *ThGH3.1* function was analyzed at the individual, genetic, and physiological levels. These findings will deepen our understanding of the molecular mechanisms regulating root development in *T. hemsleyanum*.

2. Materials and Methods

2.1. Plant Materials

Plantlets of *T. hemsleyanum* were maintained in the tissue culture laboratory of Hangzhou Normal University, Hangzhou, Zhejiang Province, China. Plantlets were cultured on Murashige & Skoog (MS) solid medium [33] and incubated at 22 ± 2 °C under 12 h photosynthetically active radiation (PAR) at $1500\text{--}2000 \mu\text{mol m}^{-2} \text{s}^{-1}$. Roots were collected for total RNA extraction, while leaves were used for hairy root induction.

Furthermore, *Arabidopsis thaliana* ecotype Columbia-0 (Col-0) was used for transformation. Homozygous T3 generation was used for all experiments.

2.2. Gene Isolation and Sequence Analysis of *ThGH3.1*

Total RNA was extracted using the FastPure Universal Plant Total RNA Isolation Kit (Vazyme, Nanjing, China) according to the manufacturer's instructions. Then, RNA was reverse transcribed to cDNA using the FastKing cDNA kit (TIANGEN, Beijing, China) in accordance with the manufacturer's instructions. The coding sequence (CDS) of *ThGH3.1* gene was amplified using gene-specific primers (Table S1). Sequencing conducted by Tsingke Biotechnology Co., Ltd. (Hangzhou, China) verified the PCR products. Sequence alignment was detected via multiple alignment analysis using DNAMAN (version 5.0). ExPASy tools (accessed on 21 May 2022) were utilized to forecast the primary structure and some basic properties of the *ThGH3.1* protein [34]. The TMHMM server was used for analyzing transmembrane domains [35]. SWISS-MODEL was used to predict tertiary structure (<https://swissmodel.expasy.org/>, accessed on 10 October 2024). Phylogenetic analysis was performed using MEGA11 software (v11) with neighbor-joining and a bootstrap repeat value of 1000 times.

2.3. Construction of *ThGH3.1* Overexpression and *ThGH3.1* RNA Interference Vectors

Recombinant vectors were constructed using the ClonExpress II One Step Cloning Kit (Vazyme Biotech Co., Ltd., Nanjing, China). In detail, the CDS of the *ThGH3.1* gene was amplified using gene-specific primers in the sense and anti-sense orientations, and then cloned into the plant expression vector pRI101-AN between *Bam*H I and *Sal* I restriction sites by homologous recombination. The primers used for fragment amplification are listed (Table S1). The resulting plasmids (*ThGH3.1*-OE, *ThGH3.1*-RNAi) were introduced into K599 *Agrobacterium* using the freeze–thaw method for subsequent analysis.

2.4. *Agrobacterium Rhizogenes*-Mediated Hairy Roots Transformation and Identification

Those recombinants (*ThGH3.1*-OE and *ThGH3.1*-RNAi) were transfected into the leaves of *T. hemsleyanum* via *A. rhizogenes* K599 to generate transgenic hairy roots, and all transformation steps followed the previous description [36]. After application of 500 mg/L cefotaxime, the bacteria-free hairy roots were propagated on B5 medium supplemented with 0.5 mg/L KT and 0.5 mg/L IBA. Two procedures were used to confirm the positive transgenic lines. First, genomic DNA was extracted from the hairy roots using the TPS method, followed by PCR amplification with gene-specific primers to identify positive lines. Primers were designed based on the *rolB* gene in the T-DNA of *A. rhizogenes* K599 and the *gfp* sequence (GenBank accession number: U17997) (Table S1). Finally, the expression levels of the *ThGH3.1* gene in transgenic lines were quantified by quantitative real-time

PCR (qRT-PCR) using SuperReal PreMix Plus Kit (TIANGEN, Beijing, China), with *GAPDH* as the internal reference gene.

2.5. Phenotype Analysis of the Transgenic Hairy Roots in *T. hemsleyanum*

Root tips were excised from wild-type (WT) and transgenic hairy roots and cultured on B5 medium supplemented with 0.5 mg/L KT and 0.5 mg/L IBA at 24 °C in the dark for 30 days. Twenty roots were collected from each group to analyze lateral root number, total root length, and root diameter using a root phenotyping system (TOP Cloud Agri Technology, Hangzhou, China).

2.6. Determination of Endogenous Phytohormones in Hairy Roots of *T. hemsleyanum*

Phytohormone contents were detected by MetWare (<http://www.metware.cn/>, accessed on 10 October 2024) using the AB Sciex QTRAP 6500 LC-MS/MS platform (SCIEX, Framingham, MA, USA). Specifically, hairy roots of *T. hemsleyanum* were ground into a homogeneous powder in liquid nitrogen, and 100 mg of each sample was used for extraction. Extraction was conducted using 1 mL of a mixed solution (methanol:acetonitrile:water = 40:20:20, *v/v*). The samples were thoroughly mixed by shaking, followed by standing at 4 °C for 12 h. After centrifugation at 12,000× *g* for 5 min, the collected supernatant was concentrated by drying with nitrogen gas. Once redissolved, the supernatant was filtered through a 0.22 µm membrane for subsequent ultra-performance liquid chromatography coupled with tandem mass spectrometry (UPLC-MS/MS) analysis according to a previously reported method [37,38].

2.7. Heterologous Expression of the *ThGH3.1* Gene in *Arabidopsis thaliana*

The constructed recombinant vector *ThGH3.1*-OE was introduced into an *Agrobacterium tumefaciens* GV3101 strain and then transformed into *A. thaliana* ecotype Columbia-0 (Col-0) using the floral dip method. After harvesting, T1-generation seeds were sown onto 1/2 MS medium containing 50 mg/L kanamycin for transformant selection. To eliminate false positives, well-grown T1 seedlings were identified by PCR using gene-specific primers. For PCR identification, genomic DNA was isolated from *A. thaliana* using the CTAB method, and PCR reactions were performed according to the Taq DNA polymerase instructions.

Furthermore, T2-generation seeds were sown on 1/2 MS medium containing 50 mg/L kanamycin to count the ratio of positive to negative seedlings. After two weeks of growth, *A. thaliana* lines exhibiting a 3:1 segregation ratio were considered single-copy insertions, which were selected and grown to maturity. Then, seeds were harvested from individual plants to obtain T3-generation seeds. Finally, T3-generation lines that grew normally were considered homozygous lines and used for subsequent analysis. Similarly, the expression level of *ThGH3.1* in *A. thaliana* was quantified by qRT-PCR with *PP2AA3* as the internal reference gene (Table S1).

2.8. Phenotype Analysis and Endogenous Phytohormones Determination of Transgenic *Arabidopsis*

Surface-sterilized wild-type (Col-0) and T3 homozygous seeds were plated on 1/2 MS medium supplemented with 50 mg/L kanamycin. After incubation at 4 °C for 3 days, the plates were transferred to constant-temperature light incubators. The specific conditions were set as follows: a 16 h light/8 h dark cycle at 22 °C, 10,000 lux light intensity, and approximately 65% relative humidity. Seedlings grown on 1/2 MS medium for 16 days were used for phenotypic analysis. After developing two true leaves, the seedlings were transplanted into plastic pots filled with nutrient soil. Then, the agronomic traits of *A. thaliana* were investigated. Additionally, their endogenous phytohormone contents were determined by MetWare (<http://www.metware.cn/>, accessed on 10 October 2024).

2.9. Evaluation of Transgenic *Arabidopsis Thaliana* in Response to IAA

To investigate the biological functions of the *ThGH3.1* gene in response to indole-3-acetic acid (IAA), hormone treatments were performed. Specifically, seeds of the WT and T3 homozygous transgenic lines were surface-sterilized with 75% ethanol and 50% bleach, then subsequently sown on half-strength Murashige and Skoog (1/2 MS) medium for 5 days. Afterward, eight seedlings with uniform growth were transferred using tweezers to fresh vertical 1/2 MS plates with different concentrations of IAA (0, 0.1, 0.5 and 1.0 mg/L). The plants were kept in a controlled environment at 22 °C with 60% relative humidity, under a 16 h light and 8 h dark photoperiod. After nine days of cultivation, primary root length was photographed and measured using Image J software (v1.8.0), and lateral root number was counted directly [39].

2.10. Statistical Analysis

Statistical analysis was performed using two-tailed Student's *t*-test via GraphPad Prism version 8 (GraphPad Software Inc., San Diego, CA, USA). Quantitative data were expressed as means \pm standard deviation (SD). Statistical significance was defined as $p < 0.05$ (*) and $p < 0.01$ (**). When comparing multiple groups, statistical significance was determined by one-way analysis of variance (ANOVA) with Tukey's multiple comparisons test. All experiments were repeated at least three times.

3. Results

3.1. Cloning and Molecular Characterization of *ThGH3.1*

In this study, qRT-PCR results show that the expression level of the *ThGH3.1* gene is highest at the calabash-shaped tuberous root stage, which is consistent with that of RNA-Seq (Figure 1A). We aim to isolate the *ThGH3.1* gene, which might be involved in root development of *T. hemsleyanum*. The full-length coding sequence of *ThGH3.1* is cloned, encoding a protein of 600 amino acids. ExPASy ProtParam analysis reveals that ThGH3.1 protein has a molecular mass of 67.591 kDa and a theoretical pI of 5.70. The protein contains 73 negatively charged residues (aspartic acid and glutamic acid) and 65 positively charged residues (specifically arginine and lysine). The overall average of hydrophobicity is calculated to be -0.274 , indicating that it is hydrophilic. The instability index of the protein is computed to be 44.77, suggesting that it is unstable. Based on TMHMM and SignalP analyses, ThGH3.1 protein does not possess signal peptides or transmembrane domains. The three-dimensional structure of ThGH3.1 protein is predicted using SWISS-MODEL (Figure 1B). As shown in Figure 1C, the secondary structure of ThGH3.1 consists of 44% alpha helices, 13.67% extended strands, and 42.33% random coils. Phylogenetic analysis of 25 GH3-related proteins from different plant species revealed that protein ThGH3.1 shared high similarity with VvGH3.1 (Figure 1D).

3.2. Induction and Identification of the Transgenic Hairy Roots in *T. hemsleyanum*

To explore *ThGH3.1* function in regulating root development, *A. rhizogenes* K599 carrying the recombinant plasmids (*ThGH3.1*-OE and *ThGH3.1*-RNAi) was used to infect the leaves of *T. hemsleyanum* seedlings (Figure 2A). After one month of growth on medium supplemented with 0.5 mg/mL kinetin, 0.5 mg/mL indole-3-butyric acid, and 500 mg/mL cefotaxime, transgenic hairy roots emerged (Figure 2B). Ultimately, large-scale propagation of transgenic hairy roots was achieved (Figure 2C–E). Positive roots were verified by PCR using *gfp*- and *rolB*-specific primers (Figure 2F). Compared to WT lines, qRT-PCR results showed a significant increase in *ThGH3.1* transcript levels in overexpression lines but a decrease in RNAi lines (Figure 2G).

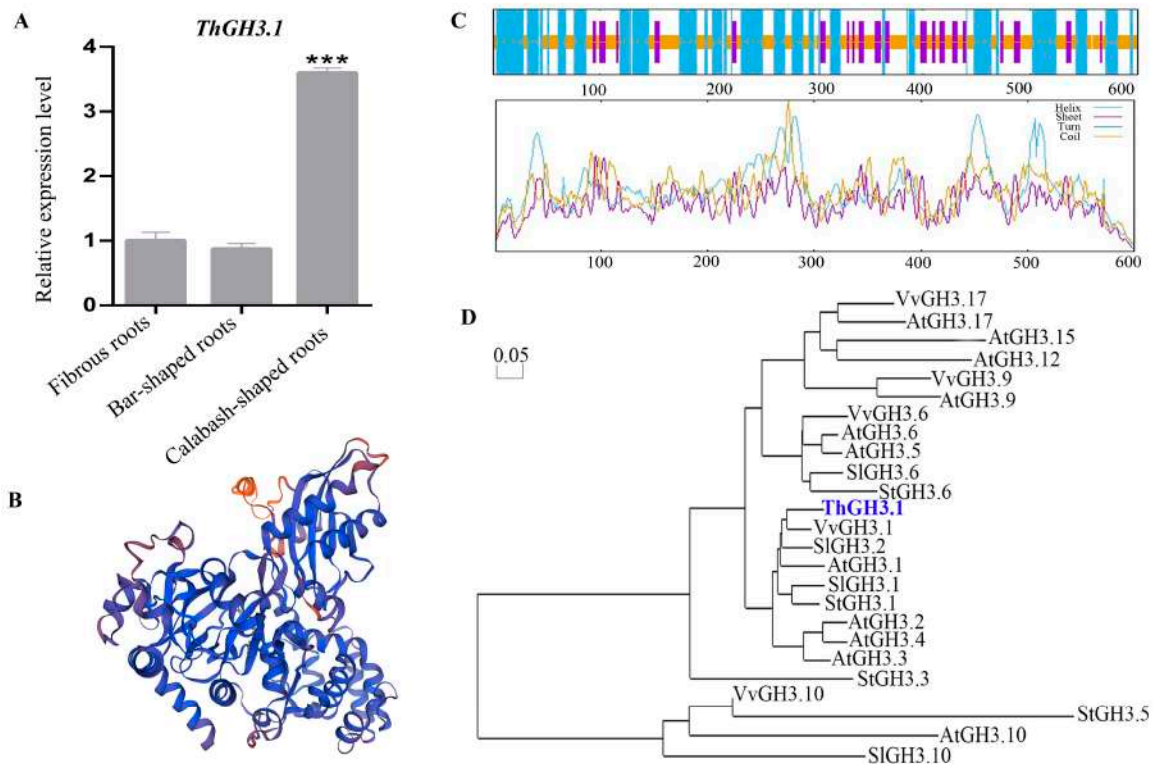


Figure 1. Expression patterns and molecular characterization of *ThGH3.1*. (A) The expression level of the *ThGH3.1* gene in fibrous roots, bar-shaped roots, and calabash-shaped tuberous roots. Data represents mean \pm SD ($n = 3$), and significant differences (***) $p < 0.001$ are based on *t*-test analysis. (B) Predicted three-dimensional structure of *ThGH3.1* protein. Each distinct colored block represents a unique protein domain. (C) Predicted secondary structure of *ThGH3.1*. (D) Phylogenetic analysis of the *ThGH3.1* alongside 25 representative GH3-related proteins from different plant species. Scale bar represents the evolutionary distance.

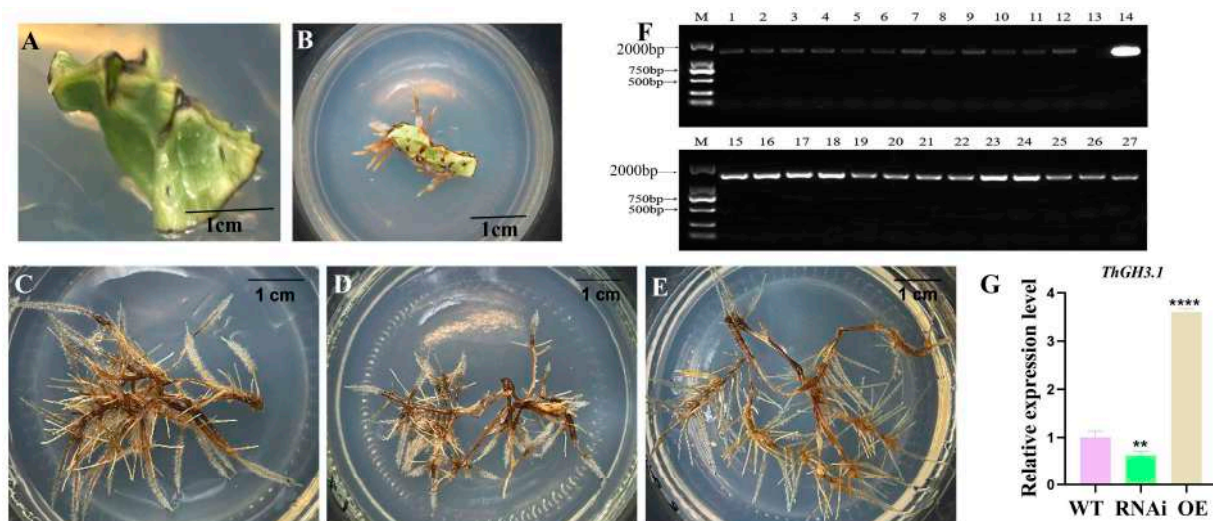


Figure 2. Induction and identification of transgenic hairy roots in *T. hemsleyanum* seedlings infected by *Agrobacterium rhizogenes* K599. (A) The infected leaves of *T. hemsleyanum*. (B) The hairy roots emerged after one month of growth on medium. (C) Large-scale propagation of hairy roots in wild-type (WT) lines. (D) Overexpression (OE) lines. (E) RNAi lines. (F) PCR confirmation of *gfp* (1–14) and *rolB* (15–27) in hairy roots. M: DL 2000 DNA molecular marker; 1–6, 15–20: OE lines; 7–12, 21–26: RNAi lines; 13, 27: non-transformed root; 14: positive control. (G) Expression level of the *ThGH3.1* gene in transgenic hairy roots and wild types (WTs). Data are expressed as the mean \pm SD ($n = 3$). Statistical significance was defined using Student's *t*-test: $p < 0.01$ (**) and $p < 0.0001$ (****).

3.3. Overexpression of *ThGH3.1* Inhibited the Total Length and Lateral Root Number of Hairy Roots and Significantly Increased Auxin Contents in *T. hemsleyanum*

After cultivation in a constant-temperature light incubator for 30 days, the transgenic hairy roots overexpressing *ThGH3.1* showed significant morphological differences compared with WT hairy roots (Figure 3A–I). The total root length and lateral root number in OE lines were significantly lower than those of the WT, whereas root diameters were similar to those of WT lines (Figure 3J–L). Additionally, the contents of endogenous phytohormones in OE lines, including Methyl indole-3-acetate (MeIAA), indole-3-acetyl-aspartate (IAA-Asp) and indole-3-pyruvic acid (IP), were significantly higher than those in the WT (Figure 3M–O). These findings suggested that overexpression of *ThGH3.1* inhibited root development in *T. hemsleyanum*.

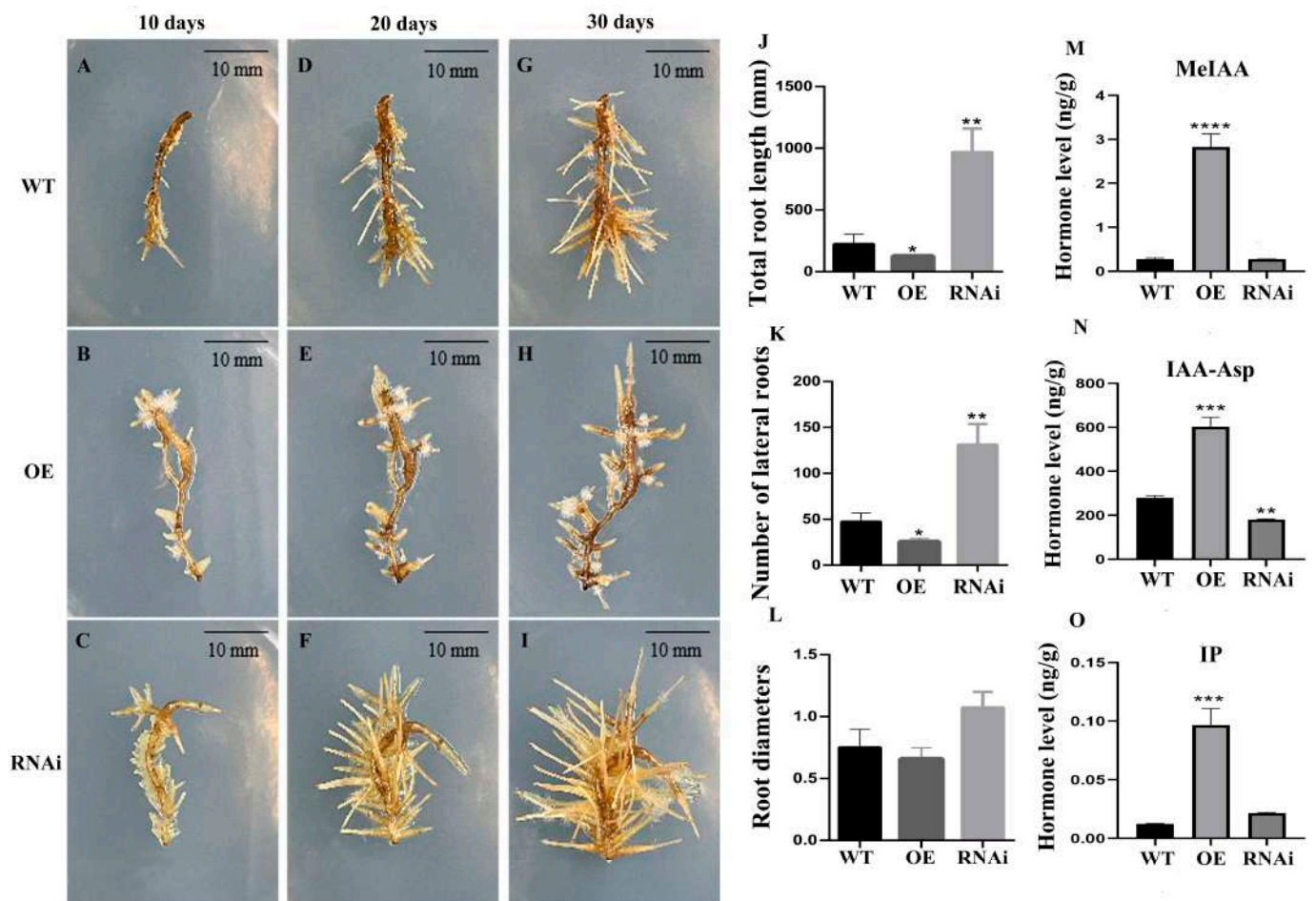


Figure 3. Overexpression and RNA interference of *ThGH3.1* in *T. hemsleyanum*. (A,D,G) WT hairy roots cultured for 10, 20, and 30 days; (B,E,H) *ThGH3.1*-overexpressing (OE) hairy roots cultured for 10, 20, and 30 days; (C,F,I) *ThGH3.1* RNA interference (RNAi) hairy roots cultured for 10, 20, and 30 days; (J–L) Total root length, lateral root number, and root diameters in the WT, OE, and RNAi hairy roots, respectively. (M–O) MeIAA, IAA-Asp, and IP content in the WT, OE, and RNAi hairy roots, respectively. Data are expressed as the mean \pm SD (n = 6). Statistical significance was defined using Student's *t*-test: $p < 0.05$ (*), $p < 0.01$ (**), $p < 0.001$ (***), and $p < 0.0001$ (****).

3.4. RNA Interference of *ThGH3.1* Promoted the Total Length and Lateral Root Number of Hairy Roots, and Significantly Decreased Auxin Contents in *T. hemsleyanum*

To further validate the function of *ThGH3.1* in regulating root development, transgenic hairy roots with *ThGH3.1* knockdown via RNA interference were generated (Figure 3A–I). The results showed that both total root length and lateral root number were significantly

higher in RNAi lines than in WT, while root diameters showed no significant differences (Figure 3J–L). In contrast to the WT, the endogenous level of IAA-Asp was significantly lower in RNAi lines, but the levels of MeIAA and IP showed no significant differences (Figure 3M–O). Similarly, these findings suggested that knockdown of *ThGH3.1* significantly promoted root development in *T. hemsleyanum*.

3.5. Acquisition of *ThGH3.1*-Overexpressing Lines and Screening of Pure Lines in Transgenic *Arabidopsis thaliana*

To obtain pure *ThGH3.1*-overexpressing *Arabidopsis* lines for subsequent phenotypic observation and functional verification, the 35S:*ThGH3.1* overexpression vector was successfully introduced into the *Agrobacterium* GV3101, and *Arabidopsis* was transformed via *Agrobacterium* inflorescence infiltration. After screening with Kanamycin, non-transformed *Arabidopsis* plants exhibited yellowing leaves and inhibited root elongation (Figure 4A). Subsequent PCR analysis showed that 34 positive T1 plants were obtained (Figure 4B). Plants exhibiting a segregation ratio of 3:1 were identified as single-copy insertions (Figure 4C). Finally, a total of five T3-generation pure lines were obtained (Figure 4D). Furthermore, the expression levels of the *ThGH3.1* gene in five pure lines were determined by qRT-PCR. The results showed that the lines G19, G29, and G32 exhibited the highest expression levels, and were thus selected as materials for subsequent experiments (Figure 4E).

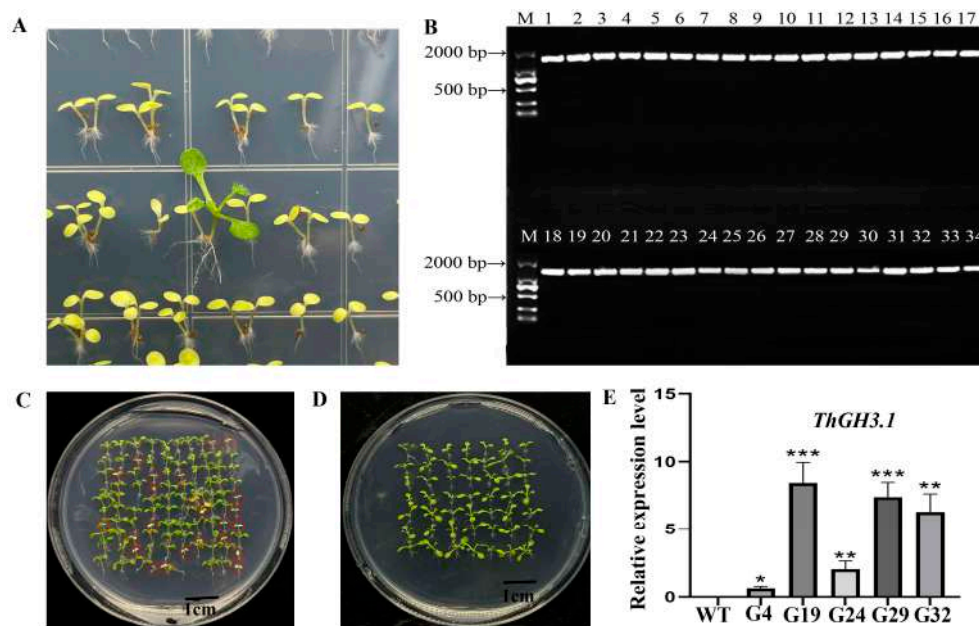


Figure 4. Screening of transgenic *Arabidopsis* pure lines and expression levels of *ThGH3.1*. (A) Screening of positive transgenic *A. thaliana* seedlings on 1/2 MS medium supplemented with 50 mg/L Kanamycin. Note: The red arrow indicates positive seedlings that can grow normally. (B) Identification of positive transgenic plants by PCR. M: DL 2000 marker; 1–34: *ThGH3.1*-transgenic *A. thaliana*. (C) Single-copy lines in *A. thaliana*. Red circles represent the negative plants. (D) Pure lines in *A. thaliana*. (E) Expression levels of the *ThGH3.1* gene in five pure transgenic *A. thaliana*. Values are means \pm SD (n = 3). Asterisks indicate significant differences (Student’s *t*-test; * $p < 0.05$, ** $p < 0.01$, *** $p < 0.001$).

3.6. Phenotypic Analysis of Transgenic *Arabidopsis thaliana* Overexpressing *ThGH3.1*

After 10 days of growth on 1/2 MS medium supplemented with 50 mg/L Kanamycin, phenotypes of WT and transgenic lines were statistically analyzed (Figure 5A). The results showed that the primary root lengths of overexpressing lines (G19 and G29) were significantly decreased (Figure 5B). The seedlings were then transplanted into soil, and the leaf

area of overexpressing lines was measured at 16 days post-transplantation (Figure 6A). The results showed that the leaf areas of overexpressing lines (G29 and G32) were significantly smaller than those of the WT (Figure 6C). In addition, the plant height of overexpressing lines was significantly shorter than that of WT lines at 30 days post-transplantation (Figure 6B,D). These findings indicated that *ThGH3.1* inhibited primary root growth in *A. thaliana*.

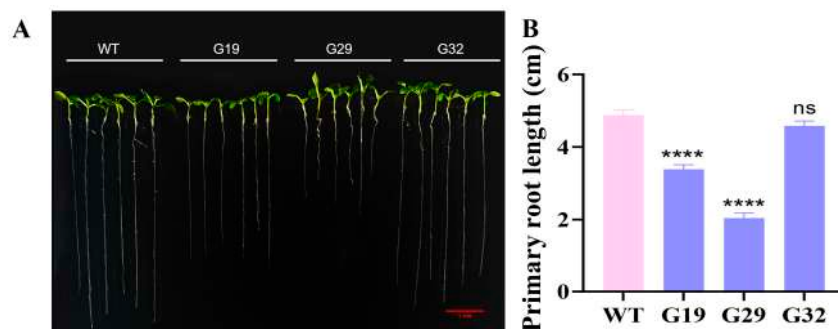


Figure 5. Morphological comparison of transgenic *Arabidopsis thaliana* overexpressing *ThGH3.1*. (A) Morphological comparison of overexpressing plants (G19, G29, and G32) and wild type (WT) *A. thaliana* grown on the medium for 16 days. (B) Primary root length of overexpressing and WT lines. Values are means \pm SD ($n = 6$). Asterisks indicate significant differences (Student's *t*-test; **** $p < 0.0001$, ns represents no significant difference).

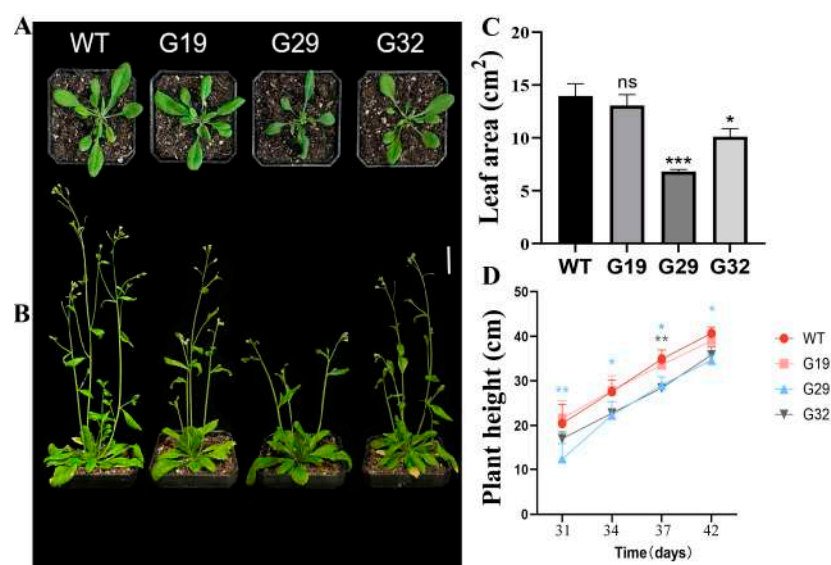


Figure 6. Phenotypic plots of wild-type (WT) and transgenic *Arabidopsis* after transplantation. (A) Growth performance of WT, G19, G29, and G32 at 16 days after transplantation. (B) Growth performance of WT, G19, G29, and G32 at 30 days after transplantation. Scale bars, 2.5 cm. (C) Leaf area of WT, G19, G29, and G32 at 16 days after transplantation. (D) Plant height of WT, G19, G29, and G32 at 30 days after transplantation. Data are statistically analyzed every 1, 4, 7, 12 days, and values are means \pm SD ($n = 6$). Asterisks indicate significant differences (Student's *t*-test; * $p < 0.05$, ** $p < 0.01$, *** $p < 0.001$, ns represents no significant difference).

3.7. Hormone Levels of Transgenic *Arabidopsis thaliana* Overexpressing *ThGH3.1*

After germination of *Arabidopsis* seeds on 1/2 MS medium, seedlings were further cultured for 7 days at 22 °C under 16 h light at 150 $\mu\text{mol m}^{-2} \text{s}^{-1}$ /8 h dark conditions. The whole seedlings of WT, G19, G29, and G32 were sampled for hormone determination. The results showed that the MeIAA levels in the overexpressing lines had no significant differences compared with those in WTs (Figure 7A). Additionally, we initially aimed to

quantify all 27 auxins in *Arabidopsis thaliana* (including IAA, ME-IAA, IBA, ICA, ICAId, IPA, IAA-GIC, IAA-Glu, IAN, IAA-Leu-Me, IAA-Leu, IAA-Phe, IAA-Glu-diMe, IAA-Val-Me, IAA-Gly, OxIAA, IAA-ASp, IAA-Val, IAA-Phe -Me, IAA-Trp, IAM, TRA, ILA, IA, IAA-Ala, TRP, and Indole) based on MetWare (<http://www.metware.cn/>, accessed on 10 October 2024) using the AB Sciex QTRAP 6500 LC-MS/MS platform (SCIEX, USA). Finally, the results showed that the IAN levels were significantly increased in all transgenic lines compared with those in WTs (Figure 7B).

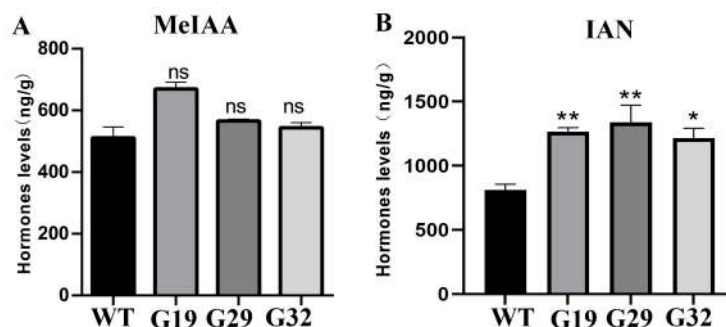


Figure 7. The phytohormone content of transgenic *Arabidopsis thaliana* overexpressing *ThGH3.1*. (A) MeIAA levels of *ThGH3.1*-OE and WT. (B) IAN levels of *ThGH3.1*-OE and WT. Data are means \pm SD (n = 3). Asterisks indicate significant differences (Student's *t*-test; * $p < 0.05$, ** $p < 0.01$, ns represents no significant difference).

3.8. Hormone Response of Transgenic *ThGH3.1*-Expressing *Arabidopsis*

To explore whether the *ThGH3.1* gene actually responds to IAA, a gradient concentration hormone assay was carried out. Under low concentration conditions (0.1 mg/L IAA), the primary root length of overexpression lines was significantly longer than that of the control group but still significantly shorter than that of the wild type (Figure 8A,B). In addition, there was no significant difference in lateral root number at 0.1 mg/L IAA (Figure 8C). At IAA concentrations of 0.5 mg/L and 1.0 mg/L, both the primary root length of WT and transgenic lines were significantly reduced compared with the control group, while the lateral root number was significantly increased (Figure 8B,C).

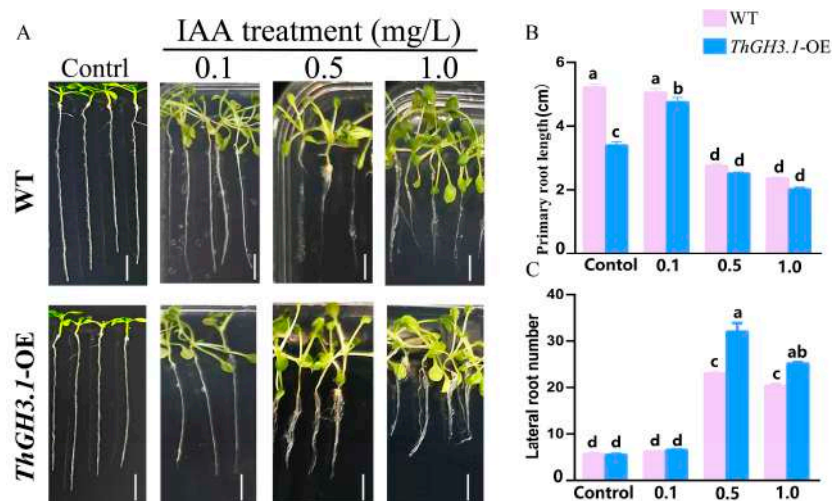


Figure 8. Hormone response of transgenic *ThGH3.1*-overexpressing *Arabidopsis*. (A) Morphological observations of WT and transgenic lines under the concentrations of 0, 0.1, 0.5, 1.0 mg/L IAA. Scale bars, 1 cm. (B) The primary root length of WT and transgenic lines under concentrations of 0, 0.1, 0.5, 1.0 mg/L IAA. (C) The lateral root numbers of WT and transgenic lines. Data are presented as mean \pm SD (n = 3). Different lowercase letters (a, b, c, d) indicate a significant difference ($p < 0.05$), determined using one-way ANOVA with Tukey's test.

4. Discussion

The *GH3* gene was first identified as an auxin-responsive gene in soybeans and has been extensively studied in model plants such as *Arabidopsis thaliana* [40]. Studies have reported that the grape *GH3.1* gene is involved in the development of plant reproductive organs, accompanied by a decrease in free IAA content and an increase in IAA-Asp content [41]. In this study, total RNA was extracted from the roots of *T. hemsleyanum*, and the reverse-transcribed cDNA was used as a template. The CDS of the *ThGH3.1* gene from *T. hemsleyanum* was successfully amplified using gene-specific primers. BLAST (<https://blast.ncbi.nlm.nih.gov/Blast.cgi>, accessed on 10 October 2024) results showed that the sequence with the highest similarity to *ThGH3.1* was the grape *VvGH3.1* (Figure 1). The above research provides a reference for the functional study of the *ThGH3.1* gene cloned in this study.

In this study, overexpressing and RNA interference vectors were constructed, and successfully induced *ThGH3.1*-overexpressing and -interfering hairy roots based on the mature hairy root genetic transformation system established by our research group (Figure 2C–E). qRT-PCR results showed that the expression level of the target gene was significantly increased in *ThGH3.1*-OE hairy roots, while it was remarkably decreased in *ThGH3.1*-RNAi hairy roots (Figure 2G). Furthermore, the role of the *GH3.1* gene in regulating plant root development was explored through phenotypic analysis and endogenous hormone determination.

Studies have shown that GH3 amide synthetases converted IAA into the IAA-amino acid conjugates IAA-Asp and IAA-Glu. Second, ILR1 amide hydrolases catalyzed the conversion of IAA-amino acid conjugates into free IAA; DAO dioxygenases oxidized IAA-amino acid conjugates, which were subsequently hydrolyzed by ILR1 to form inactive ox-IAA. The plant hormone IAA maintained auxin homeostasis through the GH3-ILR1-DAO enzymatic pathway involving storage, activation, and inactivation, thereby regulating plant growth and development [23,42]. When low concentrations of exogenous IAA were applied, the expression of the *Arabidopsis AtGH3.9* gene was inhibited. Under high IAA concentration conditions, the expression level of the *GH3.9* gene remained unaffected and the *GH3.9*-RNAi lines exhibited longer primary roots [24]. Knockout mutants of *Arabidopsis AtGH3.3*, *AtGH3.5*, and *AtGH3.6* exhibited an increased number of adventitious roots and longer primary roots, presumably due to elevated content of endogenous free IAA [21]. In addition, overexpression of *CsGH3.4* in tea plants significantly reduced free IAA content, while inhibition of *CsGH3.4* expression markedly increased free IAA content. The number of adventitious roots in *Arabidopsis* transgenic lines overexpressing *CsGH3.4* was significantly decreased, and the application of exogenous NAA can restore the number of adventitious roots in these overexpression lines [31]. Silencing of early auxin responsive genes *MdGH3-2/12* inhibited plant biomass accumulation and exacerbated root damage and ultimately reduced resistance to *Fusarium solani* in apples [43]. *SIGH3.4* is an acyl acid amino synthetase that conjugates amino acids to IAA. Disruption of such an auxin balance by the increased expression of *SIGH3.4* or *SIGH3.2* resulted in defective locular and placental tissues [44]. In our study, the total root length and lateral root number in *ThGH3.1*-RNAi hairy roots of *T. hemsleyanum* were significantly increased, while the content of the IAA-amino acid conjugate IAA-Asp was significantly decreased (Figure 3). Compared with the wild type, *ThGH3.1*-OE hairy roots showed significantly reduced total root length and lateral root number (Figure 3), but the contents of MEIAA and IAA-Asp were significantly increased (Figure 3). It was speculated that inhibiting *ThGH3.1* expression in *T. hemsleyanum* increased free IAA content and decreased conjugated IAA content, thereby promoting root elongation and lateral root development. Overexpression of *ThGH3.1* generated sufficient free IAA to inhibit hairy root growth. Similarly, overexpression of *ThGH3.1* reduced

primary root length in *Arabidopsis* but did not significantly alter MeIAA levels (Figure 7A). This phenotypic pattern in *Arabidopsis* differs from that observed in *T. hemsleyanum*, a discrepancy that may be attributed to species differences. On the other hand, it has been reported that the *rolB* gene interferes with the plant's own auxin biosynthesis or metabolic pathways, indirectly altering endogenous auxin levels, thereby regulating plant growth and development [45,46]. Collectively, it might suggest that *ThGH3.1* regulates auxin levels to affect the growth of *T. hemsleyanum* hairy roots as well as the *rolB* gene. In summary, these findings highlight the crucial roles of *ThGH3.1* in regulating root development, which will deepen our understanding of the molecular mechanisms underlying root development in plants.

Supplementary Materials: The following supporting information can be downloaded at: <https://www.mdpi.com/article/10.3390/horticulturae11121512/s1>, Table S1 The primers used in this study.

Author Contributions: Conceptualization, X.H. and H.Y.; data curation, L.W. and T.X.; formal analysis, Z.Y., Z.Z., Z.C. and T.C.; funding acquisition, X.H. and L.W.; investigation, Z.Y., Z.Z., Z.C. and T.C.; methodology, H.Y., J.J., R.Z. and F.L.; project administration, X.H.; resources, L.W. and T.X.; software, J.J., R.Z. and F.L.; supervision, X.H. and T.X.; writing—original draft, X.H. and H.Y.; writing—review and editing, X.H. All authors have read and agreed to the published version of the manuscript.

Funding: The research was funded by the Research Start-up Funds from the Hangzhou Normal University (grant number 2021QDL062), Zhejiang Regional Trial Station Project (2024QYZYC03), and Interdisciplinary Research Project of Hangzhou Normal University (2025JCXK01).

Data Availability Statement: The original contributions presented in this study are included in the article/Supplementary Material. Further inquiries can be directed to the corresponding author.

Conflicts of Interest: The authors declare no conflicts of interest.

References

- Feng, Z.; Ye, W.; Feng, L. Bioactives and metabolites of *Tetrastigma hemsleyanum* root extract alleviate DSS-induced ulcerative colitis by targeting the SYK protein in the B cell receptor signaling pathway. *J. Ethnopharmacol.* **2024**, *322*, 117563. [CrossRef]
- Wang, Y.; Jiang, W.; Ye, W.; Fu, C.; Gitzendanner, M.A.; Soltis, P.S.; Soltis, D.E.; Qiu, Y. Evolutionary insights from comparative transcriptome and transcriptome-wide coalescence analyses in *Tetrastigma hemsleyanum*. *BMC Plant Biol.* **2018**, *18*, 208. [CrossRef]
- Yuan, L.X.; Wu, H.; Peng, X.; Qiu, D.; Tao, Z.F.; Qiu, W.Y. Reference genes selection and system establishment for RT-qPCR of *T. hemsleyanum* in root development stages. *Mol. Plant Breed.* **2020**, *18*, 6785–6792. (In Chinese)
- Yan, J.; Qian, L.; Zhu, W.; Qiu, J.; Lu, Q.; Wang, X.; Wu, Q.; Ruan, S.; Huang, Y. Integrated analysis of the transcriptome and metabolome of purple and green leaves of *Tetrastigma hemsleyanum* reveals gene expression patterns involved in anthocyanin biosynthesis. *PLoS ONE* **2020**, *15*, e0230154. [CrossRef]
- Xiang, T.; Tong, X.; Li, J.; Xu, Z.; Zhou, X.; Bao, S.; Li, C. Effect of rhizosphere soil on flavonoid metabolism in roots of *Tetrastigma hemsleyanum*. *Pak. J. Agric. Sci.* **2020**, *57*, 615–622.
- Song, Y.; Wu, P.; Li, Y.; Tong, X.; Zheng, Y.; Chen, Z.; Wang, L.; Xiang, T. Effect of endophytic fungi on the host plant growth, expression of expansin gene and flavonoid content in *Tetrastigma hemsleyanum* Diels & Gilg ex Diels. *Plant Soil* **2017**, *417*, 393–402. [CrossRef]
- Zierer, W.; Rüscher, D.; Sonnwald, U.; Sonnwald, S. Tuber and tuberous root development. *Annu. Rev. Plant Biol.* **2021**, *72*, 551–580. [CrossRef] [PubMed]
- Chen, K.H.; Xing, W.; Wang, H.; Chu, M.Y.; Liu, D.L. Development and bulking mechanism of storage organs in root and tuber crops. *Plant Physiol. J.* **2024**, *60*, 1726–1736. (In Chinese)
- Wu, Y.; Jin, X.; Wang, L.; Lei, J.; Chai, S.; Wang, C.; Zhang, W.; Yang, X. Integrated transcriptional and metabolomic analysis of factors influencing root tuber enlargement during early sweet potato development. *Genes* **2024**, *15*, 1319. [CrossRef] [PubMed]
- Kondhare, K.R.; Kumar, A.; Patil, N.S.; Malankar, N.N.; Saha, K.; Banerjee, A.K. Development of aerial and belowground tubers in potato is governed by photoperiod and epigenetic mechanism. *Plant Physiol.* **2021**, *187*, 1071–1086. [CrossRef]
- Bao, X.; Zhu, Y.; Li, G.; Liu, L. Regulation of storage organ formation by long-distance tuberigen signals in potato. *Hortic. Res.* **2025**, *12*, uhae360. [CrossRef]

12. Nicolas, M.; Torres-Pérez, R.; Wahl, V.; Cruz-Oró, E.; Rodríguez-Buey, M.L.; Zamarreño, A.M.; Martín-Jouve, B.; García-Mina, J.M.; Oliveros, J.C.; Prat, S.; et al. Spatial control of potato tuberization by the TCP transcription factor Branched1b. *Nat. Plants* **2022**, *8*, 281–294. [[CrossRef](#)]
13. Noh, S.A.; Lee, H.S.; Huh, E.J.; Huh, G.H.; Paek, K.H.; Shin, J.S.; Bae, J.M. SRD1 is involved in the auxin-mediated initial thickening growth of storage root by enhancing proliferation of metaxylem and cambium cells in sweet potato (*Ipomoea batatas*). *J. Exp. Bot.* **2010**, *61*, 1337–1349. [[CrossRef](#)]
14. Noh, S.A.; Lee, H.S.; Huh, G.H.; Oh, M.J.; Paek, K.H.; Shin, J.S.; Bae, J.M. A sweet potato SRD1 promoter confers strong root-, taproot-, and tuber-specific expression in *Arabidopsis*, carrot, and potato. *Transgenic Res.* **2012**, *21*, 265–278. [[CrossRef](#)]
15. Roumeliotis, E.; Kloosterman, B.; Oortwijn, M.; Kohlen, W.; Bouwmeester, H.J.; Visser, R.G.; Bachem, C.W. The effects of auxin and strigolactones on tuber initiation and stolon architecture in potato. *J. Exp. Bot.* **2012**, *63*, 4539–4547. [[CrossRef](#)]
16. Yuan, H.; Zhao, K.; Lei, H.; Shen, X.; Liu, Y.; Liao, X.; Li, T. Genome-wide analysis of the GH3 family in apple (*Malus × domestica*). *BMC Genom.* **2013**, *14*, 297. [[CrossRef](#)]
17. Jeong, J.; Park, S.; Im, J.H.; Yi, H. Genome-wide identification of GH3 genes in *Brassica oleracea* and identification of a promoter region for anther-specific expression of a GH3 gene. *BMC Genom.* **2021**, *22*, 22. [[CrossRef](#)]
18. Zou, W.; Lin, P.; Zhao, Z.; Wang, D.; Qin, L.; Xu, F.; Su, Y.; Wu, Q.; Que, Y. Genome-wide identification of auxin-responsive GH3 gene family in *Saccharum* and the expression of *ScGH3-1* in stress response. *Int. J. Mol. Sci.* **2022**, *23*, 12750. [[CrossRef](#)] [[PubMed](#)]
19. Nakazawa, M.; Yabe, N.; Ichikawa, T.; Yamamoto, Y.Y.; Yoshizumi, T.; Hasunuma, K.; Matsui, M. *DFL1*, an auxin-responsive GH3 gene homologue, negatively regulates shoot cell elongation and lateral root formation, and positively regulates the light response of hypocotyl length. *Plant J.* **2001**, *25*, 213–221. [[CrossRef](#)] [[PubMed](#)]
20. Takase, T.; Nakazawa, M.; Ishikawa, A.; Kawashima, M.; Ichikawa, T.; Takahashi, N.; Shimada, H.; Manabe, K.; Matsui, M. *ydK1-D*, an auxin-responsive GH3 mutant that is involved in hypocotyl and root elongation. *Plant J.* **2004**, *37*, 471–483. [[CrossRef](#)] [[PubMed](#)]
21. Gutierrez, L.; Mongelard, G.; Floková, K.; Pacurar, D.I.; Novák, O.; Staswick, P.; Kowalczyk, M.; Pacurar, M.; Demailly, H.; Geiss, G.; et al. Auxin controls *Arabidopsis* adventitious root initiation by regulating jasmonic acid homeostasis. *Plant Cell* **2012**, *24*, 2515–2527. [[CrossRef](#)]
22. Sherp, A.M.; Westfall, C.S.; Alvarez, S.; Jez, J.M. *Arabidopsis thaliana* GH3.15 acyl acid amido synthetase has a highly specific substrate preference for the auxin precursor indole-3-butyric acid. *J. Biol. Chem.* **2018**, *293*, 4277–4288. [[CrossRef](#)]
23. Hayashi, K.I.; Arai, K.; Aoi, Y.; Tanaka, Y.; Hira, H.; Guo, R.; Hu, Y.; Ge, C.; Zhao, Y.; Kasahara, H.; et al. The main oxidative inactivation pathway of the plant hormone auxin. *Nat. Commun.* **2021**, *12*, 6752. [[CrossRef](#)]
24. Khan, S.; Stone, J.M. *Arabidopsis thaliana* GH3.9 influences primary root growth. *Planta* **2007**, *226*, 21–34. [[CrossRef](#)]
25. Ding, X.; Cao, Y.; Huang, L.; Zhao, J.; Xu, C.; Li, X.; Wang, S. Activation of the indole-3-acetic acid-amido synthetase GH3-8 suppresses expansin expression and promotes salicylate- and jasmonate-independent basal immunity in rice. *Plant Cell* **2008**, *20*, 228–240. [[CrossRef](#)] [[PubMed](#)]
26. Zhang, S.; Li, C.; Cao, J.; Zhang, Y.; Zhang, S.; Xia, Y.; Sun, D.; Sun, Y. Altered architecture and enhanced drought tolerance in rice via the down-regulation of indole-3-acetic acid by TLD1/OsGH3.13 activation. *Plant Physiol.* **2009**, *151*, 1889–1901. [[CrossRef](#)] [[PubMed](#)]
27. Du, H.; Wu, N.; Fu, J.; Wang, S.; Li, X.; Xiao, J.; Xiong, L. A GH3 family member, *OsGH3-2*, modulates auxin and abscisic acid levels and differentially affects drought and cold tolerance in rice. *J. Exp. Bot.* **2012**, *63*, 6467–6480. [[CrossRef](#)] [[PubMed](#)]
28. Li, X.; Yang, D.; Sun, L.; Li, Q.; Mao, B.; He, Z. The systemic acquired resistance regulator *OsNPR1* attenuates growth by repressing auxin signaling through promoting IAA-amido synthase expression. *Plant Physiol.* **2016**, *172*, 546–558. [[CrossRef](#)]
29. Ai, G.; Huang, R.; Zhang, D.; Li, M.; Li, G.; Li, W.; Ahiakpa, J.K.; Wang, Y.; Hong, Z.; Zhang, J. *SIGH3.15*, a member of the GH3 gene family, regulates lateral root development and gravitropism response by modulating auxin homeostasis in tomato. *Plant Sci.* **2023**, *330*, 111638. [[CrossRef](#)]
30. Zhao, D.; Wang, Y.; Feng, C.; Wei, Y.; Peng, X.; Guo, X.; Guo, X.; Zhai, Z.; Li, J.; Shen, X.; et al. Overexpression of *MsGH3.5* inhibits shoot and root development through the auxin and cytokinin pathways in apple plants. *Plant J.* **2020**, *103*, 166–183. [[CrossRef](#)]
31. Wang, W.; Jiao, M.; Huang, X.; Liang, W.; Ma, Z.; Lu, Z.; Tian, S.; Gao, X.; Fan, L.; He, X.; et al. The auxin-responsive *CsSPL9-CsGH3.4* module finely regulates auxin levels to suppress the development of adventitious roots in tea (*Camellia sinensis*). *Plant J.* **2024**, *119*, 2273–2287. [[CrossRef](#)]
32. Xiang, T.H.; Li, J.S.; Bao, S.Y.; Xu, Z.X.; Wang, L.Z.; Long, F.Z.; He, C.J. Digital RNA-seq transcriptome plus tissue anatomy analyses reveal the developmental mechanism of the calabash-shaped root in *Tetrastigma hemsleyanum*. *Tree Physiol.* **2021**, *41*, 1729–1748. [[CrossRef](#)]
33. Murashige, T.; Skoog, F. A revised medium for the rapid growth and bio assays with tobacco tissue cultures. *Physiol. Plant* **1962**, *15*, 473–497. [[CrossRef](#)]
34. Duvaud, S.; Gabella, C.; Lisacek, F.; Stockinger, H.; Ioannidis, V.; Durinx, C. Expasy, the Swiss Bioinformatics Resource Portal, as designed by its users. *Nucleic Acids Res.* **2021**, *49*, W216–W227. [[CrossRef](#)]

35. Moller, S.; Croning, M.D.; Apweiler, R. Evaluation of methods for the prediction of membrane spanning regions. *Bioinformatics* **2001**, *17*, 646–653. [[CrossRef](#)]
36. Du, S.; Xiang, T.; Song, Y.; Huang, L.; Sun, Y.; Han, Y. Transgenic hairy roots of *Tetrastigma hemsleyanum*: Induction, propagation, genetic characteristics and medicinal components. *Plant Cell Tiss. Org.* **2015**, *122*, 373–382. [[CrossRef](#)]
37. Pan, X.Q.; Welti, R.; Wang, X.M. Quantitative analysis of major plant hormones in crude plant extracts by high-performance liquid chromatography-mass spectrometry. *Nat. Protoc.* **2010**, *5*, 986–992. [[CrossRef](#)] [[PubMed](#)]
38. Niu, Q.F.; Zong, Y.; Qian, M.J. Simultaneous quantitative determination of major plant hormones in pear flowers and fruit by UPLC/ESI-MS/MS. *Anal. Methods* **2014**, *6*, 1766–1773. [[CrossRef](#)]
39. Sun, Y.; Yang, Z.; Zhang, C.; Xia, J.; Li, Y.; Liu, X.; Sun, L.; Tan, S. Indole-3-propionic acid regulates lateral root development by targeting auxin signaling in *Arabidopsis*. *iScience* **2024**, *27*, 110363. [[CrossRef](#)]
40. Yuan, Y.; Enhebayaer Qi, Y.H. Research Advances in Biological Functions of GH3 Gene Family in Plants. *Chin. Bull. Bot.* **2023**, *58*, 770–782. (In Chinese)
41. Böttcher, C.; Keyzers, R.A.; Boss, P.K.; Davies, C. Sequestration of auxin by the indole-3-acetic acid-amido synthetase GH3-1 in grape berry (*Vitis vinifera* L.) and the proposed role of auxin conjugation during ripening. *J. Exp. Bot.* **2010**, *61*, 3615–3625. [[CrossRef](#)] [[PubMed](#)]
42. Luo, P.; Li, T.; Shi, W.; Ma, Q.; Di, D. The roles of Gretchen Hagen 3 (GH3)-dependent auxin conjugation in the regulation of plant development and stress adaptation. *Plants* **2023**, *12*, 4111. [[CrossRef](#)]
43. Liu, Q.; Xu, S.; Jin, L.; Yu, X.; Yang, C.; Liu, X.M.; Zhang, Z.J.; Liu, Y.S.; Li, C.; Ma, F.W. Silencing of early auxin responsive genes MdGH3-2/12 reduces the resistance to *Fusarium solani* in apple. *J. Integr. Agr.* **2024**, *23*, 3012–3024. [[CrossRef](#)]
44. Hua, B.; Wu, J.Q.; Han, X.Q.; Bian, X.X.; Xu, Z.J.; Sun, C.; Wang, R.Y.; Zhang, W.Y.; Liang, F.; Zhang, H.M.; et al. Auxin homeostasis is maintained by *sly-miR167-SLARF8A/B-SIGH3.4* feedback module in the development of locular and placental tissues of tomato fruits. *New Phytol.* **2023**, *241*, 1177–1192. [[CrossRef](#)]
45. Shkryl, Y.; Vasyutkina, E.; Gorpenchenko, T.; Mironova, A.A.; Rusapetova, T.V.; Velansky, P.V.; Bulgakov, V.P.; Yugay, Y.A. Salicylic acid and jasmonic acid biosynthetic pathways are simultaneously activated in transgenic *Arabidopsis* expressing the *rolB/C* gene from *Ipomoea batatas*. *Plant Physiol. Biochem.* **2024**, *208*, 108521. [[CrossRef](#)] [[PubMed](#)]
46. Lore, G.; Evi, C.; Nicolás, P.M.; Jhon, V.M.; Ana Cristina, J.M.; Savio, D.R.; Liesbeth, D.M.; Veronique, J.; Marc, V.M.; Barbara, D.C.; et al. *Rhizogenic Agrobacterium* protein RolB interacts with the TOPLESS repressor proteins to reprogram plant immunity and development. *Proc. Natl. Acad. Sci. USA* **2023**, *120*, e2210300120.

Disclaimer/Publisher’s Note: The statements, opinions and data contained in all publications are solely those of the individual author(s) and contributor(s) and not of MDPI and/or the editor(s). MDPI and/or the editor(s) disclaim responsibility for any injury to people or property resulting from any ideas, methods, instructions or products referred to in the content.